

## Article

# Design of Cu–Cr Alloys with High Strength and High Ductility Based on First-Principles Calculations

Huihui Xiong <sup>1,2</sup> , Yingying Ma <sup>1</sup>, Haihui Zhang <sup>1,\*</sup>  and Liyong Chen <sup>1</sup>

<sup>1</sup> Faculty of Materials, Metallurgy and Chemistry, Jiangxi University of Science and Technology, Ganzhou 341000, China

<sup>2</sup> Jiangxi Advanced Copper Industry Research Institute, Yingtan 335400, China

\* Correspondence: zhanghaihuiemail@gmail.com

**Abstract:** Designing a material to realize the simultaneous improvement in strength and ductility is very meaningful to its industrial application. Here, the first-principles calculations based on density functional theory (DFT) were adopted to investigate the stability, elastic properties and Debye temperature of binary Cu–Cr alloys; and the effect of micro-alloying elements on their mechanical properties, including the bulk modulus  $B$ , shear modulus  $G$ , Yong’s modulus  $E$  and Poisson’s ratio  $\sigma$ , was discussed. The elastic constants show that all the studied binary Cu–Cr alloys are mechanically stable, and the Cu–0.7Cr alloy has a combination of good strength and ductility. Moreover, the addition of Ag, Sn, Nb, Ti and Zr can improve the basic properties of Cu–0.7Cr alloy, and the Cu–0.7Cr–1.1Sn possess a large strength combined with improved ductility and strong covalent bonds due to the large Debye temperature. Additionally, the introduction of Y and In further improves the mechanical properties (strength and ductility) of the excellent Cu–0.7Cr–1.1Sn alloy. Our studied results can provide guidance for the theoretical design and experimental improvement of Cu-based alloys.

**Keywords:** Cu–Cr alloy; DFT calculation; composition design; strength and ductility



**Citation:** Xiong, H.; Ma, Y.; Zhang, H.; Chen, L. Design of Cu–Cr Alloys with High Strength and High Ductility Based on First-Principles Calculations. *Metals* **2022**, *12*, 1406. <https://doi.org/10.3390/met12091406>

Academic Editor: Alain Pasturel

Received: 31 July 2022

Accepted: 23 August 2022

Published: 25 August 2022

**Publisher’s Note:** MDPI stays neutral with regard to jurisdictional claims in published maps and institutional affiliations.



**Copyright:** © 2022 by the authors. Licensee MDPI, Basel, Switzerland. This article is an open access article distributed under the terms and conditions of the Creative Commons Attribution (CC BY) license (<https://creativecommons.org/licenses/by/4.0/>).

## 1. Introduction

Due to their excellent strength, plasticity and conductivity, the Cu–Cr alloys have been widely used in the railway transportation industries [1], electrode materials [2] and even ultra-large-scale integrated circuit lead frames [3–5], but the industrial application of binary Cu–Cr alloy is limited because of the poor softening resistance at high temperatures, which is caused by the unstable and coarsening Cr precipitate of Cu matrix during aging treatment [3,6]. To further improve the mechanical properties of binary Cu–Cr alloys, the micro-alloying elements are added to the Cu matrix [7,8]. For instance, Xiao et al. [9] found that the introduction of trace Ca and Sr could obviously improve the softening resistance of Cu–0.57Cr alloy; the high-density dislocations and fine Cr precipitates resulted in the high strengths of Cu–Cr–Ca and Cu–Cr–Sr alloys. Additionally, adding 0.28 wt% Ti into Cu–0.45Cr alloy can inhibit its recrystallization and increase the softening temperature of this alloy [10]. Moreover, Sn addition can realize the simultaneous improvement in yield strength and electrical conductivity of Cu–0.67Cr alloy [11]. Apart from those micro-alloying elements, the introduction of Nb, Mg, Zr and Hf was also demonstrated to improve the comprehensive properties of binary Cu–Cr alloys [12–15].

Currently, many researchers also employ the experimental method to study the feasibility and effectiveness of adding noble metal and rare earth (RE) into Cu–Cr alloys. For example, Xie et al. [4] reported that a small amount of Ag could enhance the solution strengthening and obviously restrict the chain precipitation of Cr precipitates for the Cu–Cr alloys and revealed that the Cu–0.89Cr alloy containing 0.44 wt% Ag had the outstanding mechanical-electrical properties. Jie et al. [5] investigated the effects of various Y content on

the mechanical properties of Cu–0.9Cr and Cu–1.45Cr alloys and found that the addition of Y could effectively refine the eutectic structure, inhibit the coarsening of Cr precipitates and increase the dislocation density, which results in the good balance of tensile strength, hardness and electrical conductivity. Moreover, the Y was also found to obviously improve the high-temperature performance of the Cu–Cr–Zr alloy, and the minor Sc, Er had a similar positive effect on the Cu–Cr–Zr alloy [16]. Additionally, the addition of Yb restricted the coarsening of Cr-rich precipitates in Cu–Cr–Yb alloy, which makes this alloy possess better softening resistance, higher strength and electrical conductivity in comparison with Cu–Cr alloy [17]. All those studies show that the microalloying method is an effective way to realize the improvement of strength and ductility.

Nowadays, the first-principles calculations based on the density functional theory (DFT) method are also an effective way to design high-performance materials, such as Fe-based alloy [18], Al-based alloy [19] and high entropy alloys [20,21]. Compared with the experimental method, the DFT computations possess the advantages of low cost, convenience and high accuracy and thus have been extensively used in the evaluation and screening of materials. For example, Vitos et al. [18] employed quantum mechanical calculations to conduct the design of austenitic stainless steels, they found that the Fe<sub>58</sub>Cr<sub>18</sub>Ni<sub>24</sub> alloy had the optimal combination of hardness, ductility and corrosion resistance, and its basic properties would be further enhanced by the addition of osmium and iridium. With the help of the DFT method, Wang et al. [22] reported that the Nd and Mn had great strengthening potentials for the Mg alloy, and the local atomic ordering strategy could be used to design the high-strength Mg alloys. Additionally, the high-performance high entropy alloys can be effectively screened by calculating elastic and mechanical properties [20]. However, there are few pieces of literature about the theoretical design of high-strength Cu–Cr alloys based on the DFT method.

In this work, the first-principles calculations were employed to study the lattice constant, elastic constant and mechanical properties of different Cu–Cr alloys. The virtual crystal approximation (VCA) approach [23] was used to construct all the Cu-based alloys models. The stability and elastic properties of binary Cu–Cr alloys were firstly calculated and analyzed. After the screening of the excellent binary Cu–Cr alloys, the different micro-alloying elements, including Ag, Sn, Nb, Ti, Zr, In and rare earth (Y, Sc, Yb), were added to this outstanding class of Cu alloys, and their elastic constants and moduli were systematically discussed. Finally, the ternary and quaternary Cu–Cr alloys with high strength and ductility were obtained. Our work can provide guidance for the theoretical design and experimental improvement of Cu-based alloys.

## 2. Calculation Method and Details

All the calculations in this work were performed by using the Cambridge Serial Total Energy Package (CASTEP) Code [24,25] based on the density functional theory (DFT). The ultra-soft pseudopotential scheme [26] was used to describe the interactions of ionic-core and valence-electrons. The exchange–correlation energy was treated by the Perdew–Burke–Ernzerh of (PBE) of generalized gradient approximation (GGA) functional [27]. The cutoff energy of plane waves was set as 500 eV for the geometry optimization and elastic properties calculations, and the k-points meshes of  $14 \times 14 \times 14$  sampled in the first irreducible Brillouin zone [28] were chosen for high accuracy. The convergence thresholds of the total energy tolerance, maximum force tolerance and maximal displacement were  $5.0 \times 10^{-6}$  eV/atom, 0.01 eV/Å, and  $5.0 \times 10^{-4}$  Å, respectively. The Broyden–Fletcher–Goldfarb–Shanno (BFGS) method was used for geometry optimization. All the Cu–Cr alloy models were built by the virtual crystal approximate (VCA) method, which was proved to be accurate enough for the disorder solid solution [23,29–31]. The calculated lattice constant of fcc-Cu in this work is 3.630 Å, which matches well with experimental data (3.636 Å) and other calculated results [32,33], indicating that our parameters are reasonable.

### 3. Results and Discussion

#### 3.1. Elastic Properties of Binary Cu–Cr Alloy

The elastic constants  $C_{ij}$  of a compound or alloy can be used to evaluate its mechanical property, which can be obtained by the stress–strain method based on the generalized Hooke’s law. For the face-centered cubic crystal, the mechanical stability follows the following conditions:

$$C_{11} > 0, C_{44} > 0, C_{11} - C_{12} > 0, C_{11} + 2C_{12} > 0 \quad (1)$$

our calculated  $C_{11}$ ,  $C_{12}$  and  $C_{44}$  of fcc-Cu are 185.16 GPa, 113.61 GPa and 79.87 GPa, which are consistent with the calculated results of Zhan [32]. Moreover, all the studied pure Cu and Cu–Cr alloys are demonstrated to meet the stability conditions. According to the elastic constants  $C_{ij}$ , the elastic properties of Cu–Cr alloys, including bulk modulus ( $B$ ), shear modulus ( $G$ ), Young’s modulus ( $E$ ) and Poisson’s ratio ( $\sigma$ ), can be determined by the Voigt–Reuss–Hill approximation:

$$B_H = B_V = B_R = \frac{1}{3}(C_{11} + 2C_{12}) \quad G_V = \frac{1}{5}(C_{11} - C_{12} + 3C_{44}) \quad G_R = \frac{5(C_{11} - C_{12})C_{44}}{4C_{44} + 3(C_{11} - C_{12})} \quad G_H = \frac{1}{2}(G_V + G_R) \quad (2)$$

$$E = \frac{9B_H G_H}{3(B_H + G_H)} \quad \sigma = \frac{3B_H - 2G_H}{2(3B_H + G_H)}$$

where the  $B_V$  and  $B_R$  are the bulk modulus calculated by Voigt and Reuss method, respectively. The  $G_V$  and  $G_R$  are the shear modulus calculated by Voigt and Reuss method, respectively.

It is well known that the solubility of Cr atom in Cu is less than 1.28 wt%; thus, the Cu-based alloys containing 0~1.3% Cr with the interval of 0.2% are taken into account, and the calculated elastic properties are summarized in Table 1. Our calculated  $B$  (137.46 GPa) and  $G$  (57.86 GPa) of pure Cu agree well with the previously reported results [34]. The  $B$  of polycrystalline alloy is often in direct proportion to the cohesive energy [35], which represents the resistance of the material to bond rupture [36], while the  $G$  of polycrystalline alloy represents the opposition of the material to plastic deformation, which can be used to evaluate the mechanical hardness of alloys in the annealed state [37,38]. Moreover, the  $B/G$  ratio is closely related to the ductility of alloys, the large (small)  $B/G$  ratios mean the ductile (brittle) alloys [36]. Figure 1 gives the calculated  $B$ ,  $G$  and  $B/G$  of various binary Cu–Cr alloys; one can see that the shear modulus gradually decreases with the increasing Cr content, and the  $B/G$  exhibits the opposite tendency, but the bulk modulus irregularly fluctuates. After comprehensive consideration, the Cu–0.7Cr alloy has a relatively large  $B$  corresponding to the large  $G$  and large  $B/G$ . Therefore, the Cu alloy containing about 0.7% Cr should have a combination of high strength, large hardness and good ductility.

**Table 1.** The calculated elastic constant ( $C_{11}$ ,  $C_{12}$  and  $C_{44}$ , GPa), Zener’s elastic anisotropy constant ( $A$ ), bulk modulus ( $B$ , GPa), shear modulus ( $G$ , GPa),  $B/G$ , Young’s modulus ( $E$ , GPa) and Poisson’s ratio ( $\sigma$ ) of different Cu–Cr alloy, where the  $A = 2C_{44}/(C_{11} - C_{12})$ .

Composition (wt%)	$C_{11}$	$C_{12}$	$C_{44}$	$A$	$B$	$G$	$B/G$	$E$	$\sigma$
Pure Cu	185.16	113.61	79.87	2.23	137.46	57.86	2.38	152.23	0.32
Cu–0.1Cr	185.56	113.33	80.88	2.24	137.41	58.52	2.35	153.74	0.31
Cu–0.3Cr	182.73	113.50	83.14	2.40	136.58	58.50	2.33	153.58	0.31
Cu–0.5Cr	176.98	117.87	83.69	2.83	137.57	55.17	2.49	146.00	0.32
Cu–0.7Cr	167.57	122.21	81.23	3.58	137.33	48.89	2.81	131.11	0.34
Cu–0.9Cr	160.45	127.30	76.46	4.61	138.35	41.89	3.30	114.14	0.36
Cu–1.1Cr	153.27	127.88	71.18	5.61	136.34	36.41	3.74	100.31	0.38
Cu–1.3Cr	150.85	129.63	66.07	6.23	136.70	32.63	4.19	90.69	0.39

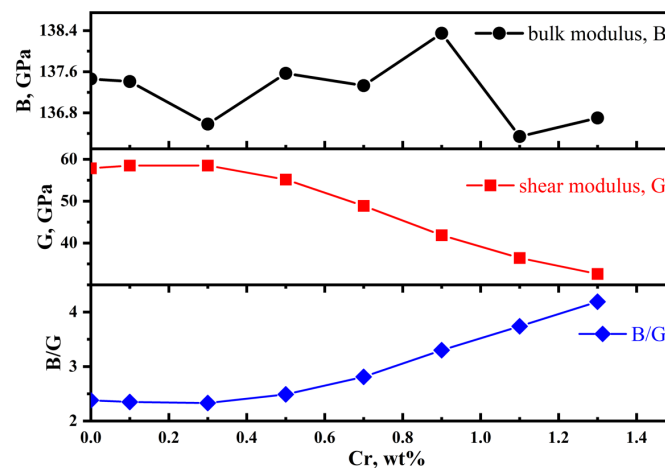


**Figure 1.** Bulk modulus, shear modulus and  $B/G$  ratios of different Cu–Cr alloys as a function of Cr content.

The Poisson ratio  $\sigma$  can be employed to estimate the degree of the covalent bond and predict the ductile or brittle of a material [39]; when the  $\sigma$  is larger than 0.26, the material has better ductility. From Table 1, the  $\sigma$  values of all the alloys are changed from 0.31 to 0.39, suggesting they exhibit good ductility characteristics. The stiffness of a material can be described by the Young's modulus, and the  $E$  greatly decreases with the increment of Cr content due to the very large decrease in shear modulus. Moreover, the Zener's elastic anisotropy constant  $A$  is in the range of 2.24~6.32. When the Cr content is more than 0.7, the  $A$  of Cu–Cr alloys is comparable and even larger than austenite stainless steel AISI 304 [18].

The Debye temperature ( $\Theta_D$ ) is closely related to many physical properties, such as the melting temperature [40], specific heat [41] and strength of covalent bonds in solids [42]. The higher  $\Theta_D$  indicates the stronger chemical bonding. The Debye temperature ( $\Theta_D$ ) can be calculated by [43]:

$$\Theta_D = \frac{h}{k_B} \left[ \frac{3n}{4\pi} \left( \frac{N_A \rho}{M} \right) \right]^{\frac{1}{3}} v_m \quad (3)$$

$$v_m = \left[ \frac{1}{3} \left( \frac{2}{v_t^3} + \frac{1}{v_l^3} \right) \right]^{-\frac{1}{3}} \quad (4)$$

$$v_l = \sqrt{\frac{(B + \frac{4}{3}G)}{\rho}} \quad v_t = \sqrt{\frac{G}{\rho}} \quad (5)$$

where  $h$ ,  $k_B$  and  $N_A$  are the Planck constant, Boltzmann constant and Avogadro constant, respectively.  $n$ ,  $M$  and  $\rho$  are the total atom numbers per formula, molecular weight per formula and theoretical density, respectively.  $v_l$  and  $v_t$  are the longitudinal sound velocity and transverse sound velocity. According to the above equations, the calculated result is Figure 2. It can be observed that the Debye temperature and theoretical density of Cu–Cr alloys gradually decreased with the increment of Cr content, indicating that the high Cr content can decrease the melting temperature and weaken the chemical bonds of Cu–Cr alloys. In particular, the chemical bond strength of Cu–Cr alloys was dramatically decreased when the Cr content was larger than 0.7%. Combining the mechanical properties and Debye temperature, the Cu–0.7Cr alloy is chosen to be further studied in the next sections.

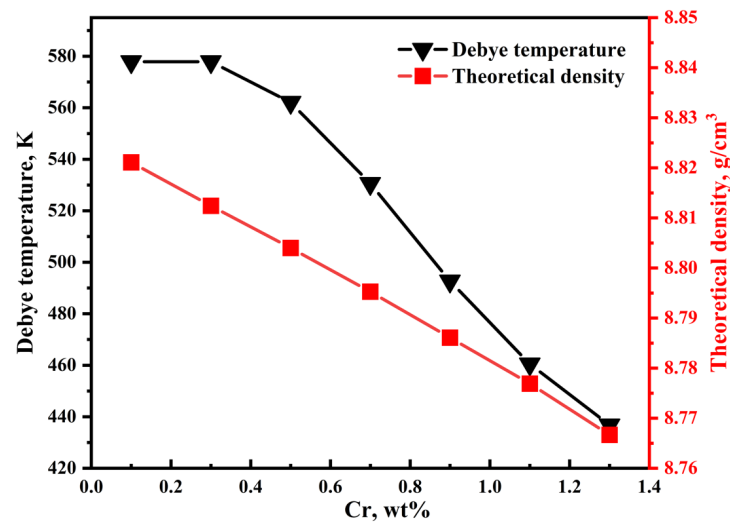


**Figure 2.** Debye temperature and theoretical density of binary Cu–Cr alloys as a function of Cr content.

### 3.2. Mechanical Properties of Ternary Cu–Cr Alloy

To improve the performance of Cu–0.7Cr alloy, the effects of the third component on its mechanical properties are investigated. The common transition metals ( $X$ ,  $X = \text{Ag, Sn, Nb, Ti}$  and  $\text{Zr}$ ) in the industrial application are taken into account. For each transition metal, 0~1.3%  $X$  with the interval of 0.2% is added into the Cu–0.7Cr alloy due to the small solubility of those elements in Cu. The calculated lattice parameters,  $B$ ,  $G$ , and  $B/G$ , of different ternary Cu–Cr alloys are shown in Figures 3 and 4. The Sn can obviously decrease the lattice parameters of Cu–0.7Cr due to the small atomic radius of Sn, while the other alloying elements have a negligible effect on it. When the Ag and Sn are introduced into the Cu–0.7Cr alloy, the  $B$ ,  $G$  and  $B/G$  are synchronously improved, and the higher Ag and Sn concentrations lead to more excellent mechanical properties, as displayed in Figure 4a,b. Moreover, the bulk modulus and shear modulus of Cu–Cr–Sn alloy is much larger than those of C–Cr–Ag alloy for the same contents, which indicates that the Cu–Cr–Sn alloys have the larger strength and mechanical hardness in comparison with Cu–Cr–Ag alloys. However, the  $B/G$  is in the range of 2.65~2.78 and 2.80~2.83 for the Cu–Cr–Sn and Cu–Cr–Ag alloys. Evidently, the Cu–Cr–Ag alloys exhibit better ductility due to the larger  $B/G$ . Hence, the Cu–0.7Cr–1.1Sn and Cu–0.7Cr–1.1Ag, which have high strength and toughness, should be the optimal compositions for the two alloys.

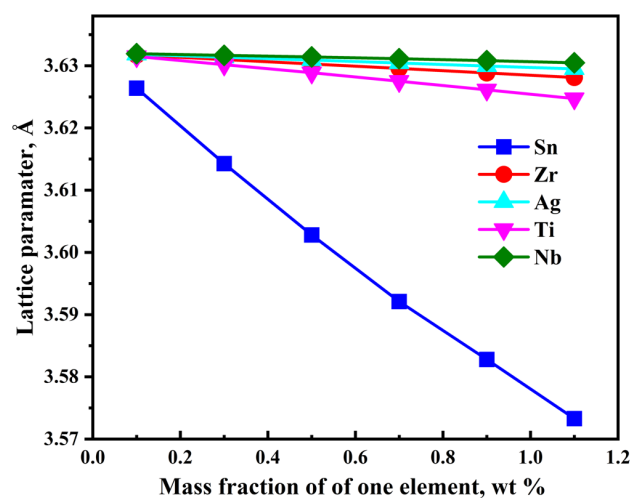


**Figure 3.** The relationship between lattice parameter of Cu–0.7Cr–X and mass fraction of alloying elements.

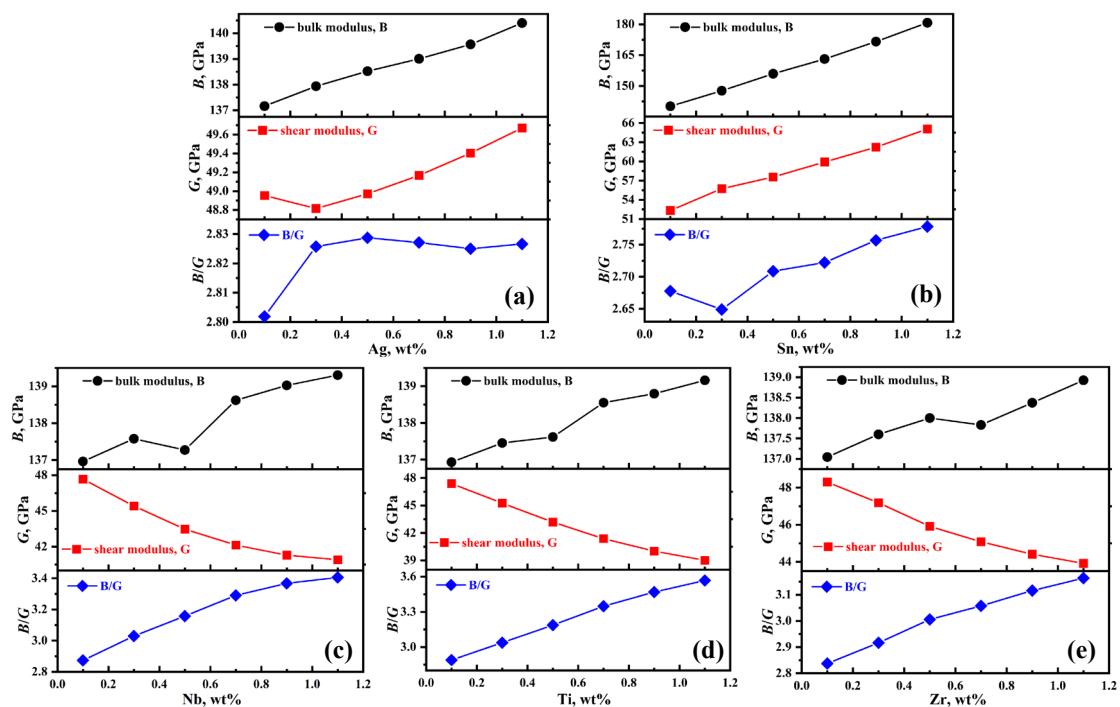


**Figure 4.** The calculated B, G and B/G ratios of different ternary Cu–Cr–X alloys as a function of X content. (a) Ag, (b) Sn, (c) Nb, (d) Ti and (e) Zr.

When the Nb, Ti and Zr are added into the Cu–0.7Cr alloy, the B, G, and B/G undergo great variations. With the increment of Nb, Ti and Zr contents, the shear modulus is gradually reduced, and the B/G shows the opposite trend, as shown in Figure 4c–e. This suggests that the large Nb, Ti and Zr concentrations are beneficial to improving the ductility of Cu–0.7Cr alloy. In addition, the bulk modulus of Cu–0.7Cr alloy exhibits the upward tendency with the increasing Nb, Ti and Zr, and the B of Cu–Cr–X (X = Nb, Ti and Zr) alloys is comparable for the same X content. By comparing the B, G, and B/G, we can find that the optimal compositions are Cu–0.7Cr–0.7Nb, Cr–0.7Cr–0.7Ti and Cu–0.7Cr–0.5Zr for the ternary Cu–Cr–Nb, Cu–Cr–Ti and Cu–Cr–Zr alloys, respectively.

In order to conduct the screening of excellent Cu-based alloys, the elastic and mechanical properties of the optimal ternary Cu–Cr–X alloys are further compared and discussed, as listed in Table 2 and Figure 5. One can see that the bulk modulus (180.76 GPa) and shear modulus (65.06 GPa) of Cu–0.7Cr–1.1Sn are much larger than those of the other alloys, suggesting that the Cu–0.7Cr–1.1Sn alloy has the largest strength and mechanical hardness. While the Cu–0.7Cr–1.1Sn alloy has a relatively small B/G value and A (Figure 5), which is much smaller than that of Cr–0.7Cr–0.7Ti. Additionally, the five ternary alloys have the comparable Poisson’s ratio  $\sigma$  (higher than 0.26), and thus, they all exhibit the feature of good ductility. Moreover, the Debye temperature  $\Theta_D$  follows the order: Cu–0.7Cr–1.1Sn > Cu–0.7Cr–1.1Ag > Cu–0.7Cr–0.5Zr > Cu–0.7Cr–0.7Nb > Cr–0.7Cr–0.7Ti. Therefore, we can conclude that the covalent bonds in Cu–0.7Cr–1.1Sn is stronger than other alloys. The  $\Theta_D$  of these alloys is smaller than that of pure Cu (574.65 K); this is because the addition of alloy elements increases the molecular weight of pure copper, as illustrated in Equation (2). Based on the above discussion, should has the optimum compositions with good mechanical properties is the Cu–0.7Cr–1.1Sn alloy, followed by the Cu–0.7Cr–1.1Ag alloy.

### 3.3. Mechanical Properties of Quaternary Cu–Cr Alloy

Based on the above discussion, the optimum ternary composition with good performance is the Cu–0.7Cr–1.1Sn. In this section, the fourth alloying elements are introduced into this alloy to further improve its mechanical properties. The calculated B, G and B/G

ratios of Cu–0.7Cr–1.1Sn alloy with different contents of In, Y, Sc and Yb are shown in Figure 6. One can see that Sc, Y and In can increase the bulk modulus of Cu–0.7Cr–1.1Sn alloy, while the Yb can slightly decrease its bulk modulus (Figure 6a). Whereas the addition of all the alloying elements can result in the increment of shear modulus for the Cu–0.7Cr–1.1Sn alloy, as depicted in Figure 6b. This implies that these alloying elements can further improve the strength and mechanical hardness, which is consistent with the experimental observation that a small amount of Y, Sc and Yb significantly improves the strength of Cu–Cr alloy [5,16,17]. In particular, the enhancement effects of Y are much more significant than that of the other elements for both B and G, and the larger Y content leads to the greater enhancement. However, most of the B/G of Cu–0.7Cr–1.1Sn alloy is decreased after the introduction of these alloying elements, meaning that its ductility is weakened to a different degree. By contrast, adding about 0.1% Y or 0.7% In can improve the ductility of the Cu–0.7Cr–1.1Sn alloy, as shown in Figure 6c, which matches well with the experimental results of Wang [5]. Therefore, the overall effect of Y or In on the Cu–0.7Cr–1.1Sn alloys realizes the goal of simultaneously increasing the bulk and shear modulus as well as B/G.

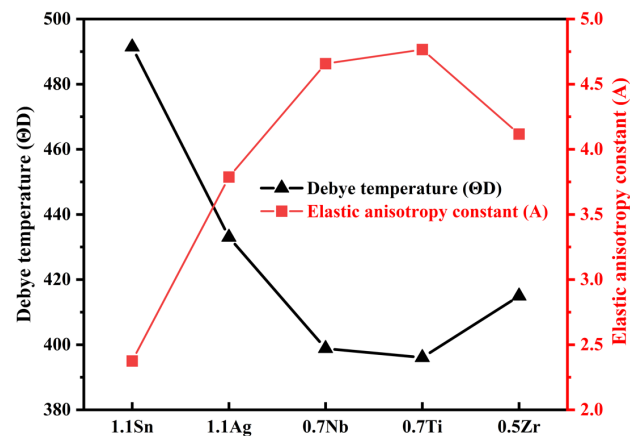


**Figure 5.** The relationship between Debye temperature, elastic anisotropy constant and different alloying contents for the optimal ternary Cu–Cr–X alloys.

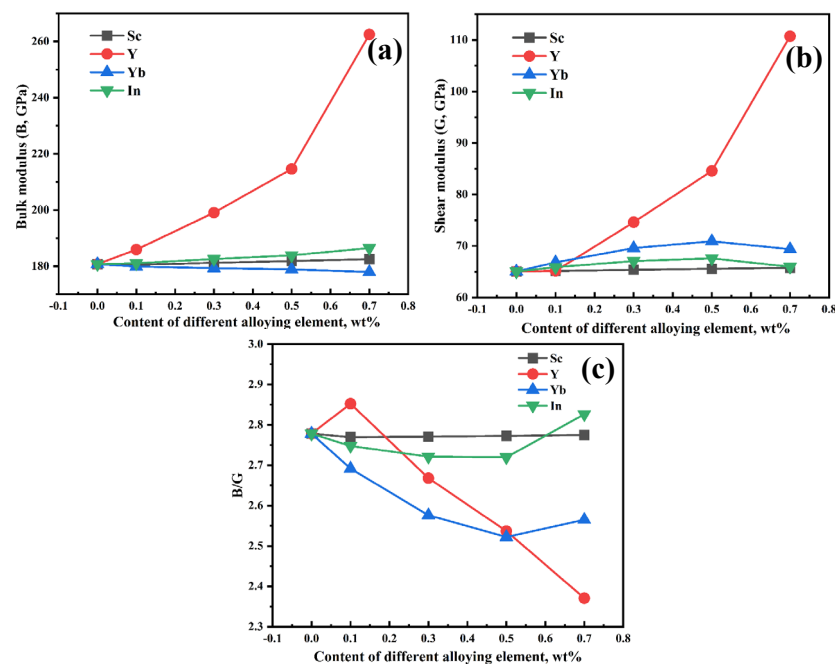


**Figure 6.** The calculated bulk modulus (a), shear modulus (b) and B/G ratios (c) of Cu–0.7Cr–1.1Sn alloy with different alloying contents.

**Table 2.** The calculated bulk modulus ( $B$ ), shear modulus ( $G$ ),  $B/G$ , Poisson's ratio ( $\sigma$ ), elastic anisotropy constant ( $A$ ) and Debye temperature ( $\Theta_D$ ) of the optimal ternary Cu–Cr–X alloys.

Composition (wt%)	$B$ , GPa	$G$ , GPa	$B/G$	$\sigma$	$A$	$\Theta_D$ , K
Cu–0.7Cr–1.1Sn	180.76	65.06	2.78	0.34	2.37	491.41
Cu–0.7Cr–1.1Ag	140.40	49.67	2.83	0.34	3.79	433.00
Cu–0.7Cr–0.7Nb	138.62	42.13	3.29	0.36	4.66	398.82
Cr–0.7Cr–0.7Ti	138.55	41.38	3.35	0.36	4.77	396.05
Cu–0.7Cr–0.5Zr	138.00	45.92	3.01	0.35	4.12	414.95

#### 4. Conclusions

In this work, the DFT method was employed to investigate the stability, elastic properties and Debye temperature of binary Cu–Cr alloys, and the effect of different alloying elements on the mechanical properties, including  $C_{ij}$ ,  $B$ ,  $G$ ,  $E$  and  $\sigma$ , of Cu-based alloys, was discussed. The results show that all the binary Cu–Cr alloys exhibit ductility characteristics, and the Cu–0.7Cr alloy has a combination of high strength, large hardness and good ductility due to the relatively large  $B$ ,  $G$  and  $B/G$ . Moreover, the addition of Ag, Sn, Nb, Ti and Zr can improve the strength and toughness of Cu–0.7Cr alloy, and the optimal compositions are Cu–0.7Cr–0.7Nb, Cr–0.7Cr–0.7Ti and Cu–0.7Cr–0.5Zr for the ternary Cu–Cr–Nb, Cu–Cr–Ti and Cu–Cr–Zr alloys, respectively. Among these ternary Cu–Cr alloys, the Cu–0.7Cr–1.1Sn has the largest strength, mechanical hardness and covalent bonds. Furthermore, the overall effect of Y or In on the Cu–0.7Cr–1.1Sn alloys realizes the goal of simultaneously increasing the bulk and shear modulus. Thus, the Cu–0.7Cr–1.1Sn alloys containing a certain Y or In should have excellent mechanical properties. Those results illustrate that the theoretical modeling of Cu alloys based on DFT computations can be an effective method in modern copper alloy design.

**Author Contributions:** H.X.: Conceptualization, methodology, investigation, writing—original draft. H.Z.: Visualization, software, data curation, supervision, writing—original draft. Y.M.: Data curation, investigation, writing—original draft. L.C.: Data curation, validation, investigation. All authors have read and agreed to the published version of the manuscript.

**Funding:** This work was financially supported by the National Natural Science Foundation of China (No. 52074135), Natural Science Foundation of Jiangxi Province (No. 20202BAB214016 and 20192BAB206020), Youth Jinggang Scholars Program in Jiangxi Province (No. QNJG2020049) and independent project of Jiangxi advanced Copper Industry Research Institute (No. ZL-202012).

**Institutional Review Board Statement:** Not applicable.

**Informed Consent Statement:** Not applicable.

**Data Availability Statement:** The data are not publicly available due to privacy.

**Conflicts of Interest:** The authors declare no conflict of interest.

#### References

- Fang, H.; Liu, P.; Chen, X.; Zhou, H.; Fu, S.; Liu, K.; Liu, H.; Guo, W. Effect of Ti addition on the microstructure and properties of Cu–Cr alloy. *Mater. Sci. Technol.* **2021**, *37*, 672–681. [[CrossRef](#)]
- Yuan, D.; Wang, J.; Chen, H.; Xie, W.; Wang, H.; Yang, B. Mechanical properties and microstructural evolution of a Cu–Cr–Ag alloy during thermomechanical treatment. *Mater. Sci. Technol.* **2018**, *34*, 1433–1440. [[CrossRef](#)]
- Guo, X.; Xiao, Z.; Qiu, W.; Li, Z.; Zhao, Z.; Wang, X.; Jiang, Y. Microstructure and properties of Cu–Cr–Nb alloy with high strength, high electrical conductivity and good softening resistance performance at elevated temperature. *Mater. Sci. Eng. A* **2019**, *749*, 281–290. [[CrossRef](#)]
- Xu, S.; Fu, H.; Wang, Y.; Xie, J. Effect of Ag addition on the microstructure and mechanical properties of Cu–Cr alloy. *Mater. Sci. Eng. A* **2018**, *726*, 208–214. [[CrossRef](#)]
- Wang, Y.; Qu, J.; Wang, X.; Jie, J.; Li, T. Effects of Y addition on the microstructure, properties and softening resistance of Cu–Cr alloy. *J. Alloys Compd.* **2022**, *902*, 163816. [[CrossRef](#)]
- Peng, L.; Xie, H.; Huang, G.; Xu, G.; Yin, X.; Feng, X.; Mi, X.; Yang, Z. The phase transformation and strengthening of a Cu–0.71 wt% Cr alloy. *J. Alloys Compd.* **2017**, *708*, 1096–1102. [[CrossRef](#)]

7. Chen, H.; Gao, P.; Peng, H.; Wei, H.; Xie, W.; Wang, H.; Yang, B. Study on the hot deformation behavior and microstructure evolution of Cu-Cr-In alloy. *J. Mater. Eng. Perform.* **2019**, *28*, 2128–2136. [[CrossRef](#)]
8. Shangina, D.V.; Bochvar, N.R.; Morozova, A.I.; Belyakov, A.N.; Kaibyshev, R.O.; Dobatkin, S.V. Effect of chromium and zirconium content on structure, strength and electrical conductivity of Cu-Cr-Zr alloys after high pressure torsion. *Mater. Lett.* **2017**, *199*, 46–49. [[CrossRef](#)]
9. Ma, M.; Xiao, Z.; Meng, X.; Li, Z.; Gong, S.; Dai, J.; Jiang, H.; Jiang, Y.; Lei, Q.; Wei, H. Effects of trace calcium and strontium on microstructure and properties of Cu-Cr alloys. *J. Mater. Sci. Technol.* **2022**, *112*, 11–23. [[CrossRef](#)]
10. Peng, H.; Xie, W.; Chen, H.; Wang, H.; Yang, B. Effect of micro-alloying element Ti on mechanical properties of Cu-Cr alloy. *J. Alloys Compd.* **2021**, *852*, 157004–157013. [[CrossRef](#)]
11. Li, J.; Ding, H.; Li, B.; Gao, W.; Bai, J.; Sha, G. Effect of Cr and Sn additions on microstructure, mechanical-electrical properties and softening resistance of Cu-Cr-Sn alloy. *Mater. Sci. Eng. A* **2021**, *802*, 140628–140637. [[CrossRef](#)]
12. Sun, Y.; Peng, L.; Huang, G.; Xie, H.; Mi, X.; Liu, X. Effects of Mg addition on the microstructure and softening resistance of Cu-Cr alloys. *Mater. Sci. Eng. A* **2020**, *776*, 139009–139019. [[CrossRef](#)]
13. Yang, X.H.; Wang, C.D.; Yang, L.; Zou, J.T.; Xiao, P.; Liang, S.H. Effects of Nb addition and different cooling methods on microstructures and properties of Cu-Cr Alloys. *J. Mater. Eng. Perform.* **2020**, *29*, 5008–5017. [[CrossRef](#)]
14. Tian, W.; Bi, L.; Ma, F.; Du, J. Effect of Zr on as-cast microstructure and properties of Cu-Cr alloy. *Vacuum* **2018**, *149*, 238–247. [[CrossRef](#)]
15. Yang, Y.; Kuang, G.; Li, R. Optimizing the electrical and mechanical properties of Cu-Cr alloys by Hf microalloying. *Metals* **2022**, *12*, 485. [[CrossRef](#)]
16. Wang, W.; Zhu, J.; Qin, N.; Zhang, Y.; Li, S.; Xiao, Z.; Lei, Q.; Li, Z. Effects of minor rare earths on the microstructure and properties of Cu-Cr-Zr alloy. *J. Alloys Compd.* **2020**, *847*, 155762–155775. [[CrossRef](#)]
17. Ma, M.; Li, Z.; Xiao, Z.; Zhu, H.; Zhang, X.; Zhao, F. Microstructure and properties of a novel Cu-Cr-Yb alloy with high strength, high electrical conductivity and good softening resistance. *Mater. Sci. Eng. A* **2020**, *795*, 140001–140009. [[CrossRef](#)]
18. Vitos, L.; Korzhavyi, P.A.; Johansson, B. Stainless steel optimization from quantum mechanical calculations. *Nat. Mater.* **2003**, *2*, 25–28. [[CrossRef](#)]
19. Zhu, A.W.; Shiflet, G.J.; Starke, E.A., Jr. First principles calculations for alloy design of moderate temperature age-hardenable Al alloys. *Mater. Sci. Forum.* **2006**, *519–521*, 35–44. [[CrossRef](#)]
20. Hu, Y.L.; Bai, L.H.; Tong, Y.G.; Deng, D.Y.; Liang, X.B.; Zhang, J.; Li, Y.J.; Chen, Y.X. First-principle calculation investigation of NbMoTaW based refractory high entropy alloys. *J. Alloys Compd.* **2020**, *827*, 153963–153970. [[CrossRef](#)]
21. Cao, P.; Ni, X.; Tian, F.; Varga, L.K.; Vitos, L. Ab initio study of Al<sub>x</sub>MoNbTiV high-entropy alloys. *J. Phys. Condens. Matter* **2015**, *27*, 075401–075408. [[CrossRef](#)] [[PubMed](#)]
22. Su, H.; Zhang, C.; Wang, S.; Tian, G.; Xue, C.; Wang, J.; Guan, S. Local atomic ordering strategy for high strength Mg alloy design by first-principle calculations. *J. Alloys Compd.* **2022**, *907*, 164491–164501. [[CrossRef](#)]
23. Bellaiche, L.; Vanderbilt, D. Virtual crystal approximation revisited: Application to dielectric and piezoelectric properties of perovskites. *Phys. Rev. B* **2000**, *61*, 7877–7882. [[CrossRef](#)]
24. Clark, S.J.; Segall, M.D.; Pickard, C.J.; Hasnip, P.J.; Probert, M.I.; Refson, K.; Payne, M.C. First principles methods using CASTEP. *Z. Krist. Cryst.* **2005**, *220*, 567–570. [[CrossRef](#)]
25. Segall, M.D.; Philip, J.D.L.; Probert, M.J.; Pickard, C.J.; Hasnip, P.J.; Clark, S.J.; Payne, M.C. First-principles simulation: Ideas, illustrations and the CASTEP code. *J. Phys. Condens. Matter* **2002**, *14*, 2717. [[CrossRef](#)]
26. Vanderbilt, D. Soft self-consistent pseudopotentials in a generalized eigenvalue formalism. *Phys. Rev. B* **1990**, *41*, 7892–7895. [[CrossRef](#)]
27. Perdew, J.P.; Burke, K.; Ernzerhof, M. Generalized gradient approximation made simple. *Phys. Rev. Lett.* **1996**, *77*, 3865–3868. [[CrossRef](#)]
28. Monkhorst, H.J.; Pack, J.D. Special points for Brillouin-zone integrations. *Phys. Rev. B* **1976**, *13*, 5188–5192. [[CrossRef](#)]
29. Winkler, B.; Pickard, C.; Milman, V. Applicability of a quantum mechanical ‘virtual crystal approximation’ to study Al/Si-disorder. *Chem. Phys. Lett.* **2002**, *362*, 266–270. [[CrossRef](#)]
30. Liao, M.; Liu, Y.; Min, L.; Lai, Z.; Han, T.; Yang, D.; Zhu, J. Alloying effect on phase stability, elastic and thermodynamic properties of Nb-Ti-V-Zr high entropy alloy. *Intermetallics* **2018**, *101*, 152–164. [[CrossRef](#)]
31. Mu, Y.; Liu, H.; Liu, Y.; Zhang, X.; Jiang, Y.; Dong, T. An ab initio and experimental studies of the structure, mechanical parameters and state density on the refractory high-entropy alloy systems. *J. Alloys Compd.* **2017**, *714*, 668–680. [[CrossRef](#)]
32. Zhang, K.; Zhan, Y. Adhesion strength and stability of Cu(111)/TiC(111) interface in composite coatings by first principles study. *Vacuum* **2019**, *165*, 215–222. [[CrossRef](#)]
33. Wu, Z.; Pang, M.; Zhan, Y.; Shu, S.; Xiong, L.; Li, Z. The bonding characteristics of the Cu(111)/WC(0001) interface: An insight from first-principle calculations. *Vacuum* **2021**, *191*, 110218. [[CrossRef](#)]
34. Kong, G.X.; Ma, X.J.; Liu, Q.J.; Li, Y.; Liu, Z.T. Structural stability, elastic and thermodynamic properties of Au-Cu alloys from first-principles calculations. *Phys. B* **2018**, *533*, 58–62. [[CrossRef](#)]
35. Gschneidner, K.A. Physical properties and interrelationships of metallic and semimetallic elements. *Solid State Phys.* **1964**, *16*, 275–426.

36. Pugh, S.F. Relations between the elastic moduli and the plastic properties of polycrystalline pure metals. *Philos. Mag.* **1954**, *45*, 823–843. [[CrossRef](#)]
37. Clerc, D.G.; Ledbetter, H.M. Mechanical hardness: A semiempirical theory based on screened electrostatics and elastic shear. *J. Phys. Chem. Solids* **1998**, *59*, 1071–1095. [[CrossRef](#)]
38. Clerc, D.G. Mechanical hardness and elastic stiffness of alloys: Semiempirical models. *J. Phys. Chem. Solids* **1999**, *60*, 83–102. [[CrossRef](#)]
39. Chen, X.; Zhang, Y.Y.; Yu, J.X. Study on Bike Rental Pricing Model under the Low-Carbon Mode. *Adv. Mater. Res.* **2011**, *299*, 1275–1278.
40. Yang, W.; Pang, M.; Tan, Y.; Zhan, Y. A comparative first-principles study on electronic structures and mechanical properties of ternary intermetallic compounds  $\text{Al}_8\text{Cr}_4\text{Y}$  and  $\text{Al}_8\text{Cu}_4\text{Y}$ : Pressure and tension effects. *J. Phys. Chem. Solids* **2016**, *98*, 298–308. [[CrossRef](#)]
41. Lv, Z.Q.; Zhang, Z.F.; Zhang, Q.; Wang, Z.H.; Sun, S.H.; Fu, W.T. Structural, electronic and elastic properties of the Laves phases  $\text{WFe}_2$ ,  $\text{MoFe}_2$ ,  $\text{WCr}_2$  and  $\text{MoCr}_2$  from first-principles. *Solid State Sci.* **2016**, *56*, 16–22. [[CrossRef](#)]
42. Zhou, Z.; Zhou, X.; Zhang, K. Phase stability, electronic structure and mechanical properties of  $\text{IrB}_x$  ( $x = 0.9, 1.1$ ): First-principles calculations. *Comp. Mater. Sci.* **2016**, *113*, 98–103. [[CrossRef](#)]
43. Farhadizadeh, A.R.; Amadeh, A.A.; Ghomi, H. The effect of metal transition dopant on electronic and mechanical properties of titanium nitride: First principle method. *Comp. Mater. Sci.* **2018**, *141*, 82–90. [[CrossRef](#)]